

# Tribenzyl Tantalum(V) Complexes of Amine Bis(phenolate) Ligands: Investigation of $\alpha$ -Abstraction vs Ligand Backbone $\beta$ -Abstraction Paths

Stanislav Groysman,<sup>†</sup> Israel Goldberg,<sup>†</sup> Moshe Kol,<sup>\*,†</sup> Elisheva Genizi,<sup>‡</sup> and Zeev Goldschmidt<sup>\*,‡</sup>

School of Chemistry, Raymond and Beverly Sackler Faculty of Exact Sciences, Tel Aviv University, Tel Aviv 69978, Israel, and Department of Chemistry, Bar-Ilan University, Ramat Gan 52900, Israel

Received January 5, 2004

The synthesis, structure, and reactivity of tribenzyl Ta(V) complexes of amine bis(phenolate) ligands were investigated as a function of the ligands' structure: i.e., the steric bulk of the phenolate substituents and the presence of a "side arm" donor. The tribenzyl complexes were prepared by toluene-elimination reactions of Ta(CH<sub>2</sub>Ph)<sub>5</sub> with the ligand precursors. They were found to be of octahedral *mer* geometry, with the side-arm donor (if present) unbound. These complexes underwent two well-defined toluene elimination reactions determined by the structural features of the ligands. An  $\alpha$ -abstraction reaction, leading to alkyl-alkylidene complexes, occurred only if the phenolate ortho substituents were small (H, Cl) and a side-arm donor was present. Bulkier phenolate substituents (Me) or the lack of a side-arm donor led to a  $\beta$ -abstraction process from the ligand backbone, forming a dibenzyl complex with a metallazacyclopropane ring. The side-arm donor, if present, was found to bind to the metal in both paths. A bulkier ligand precursor having *t*-Bu groups on the two phenolate rings did not react with Ta(CH<sub>2</sub>Ph)<sub>5</sub> at room temperature, whereas an asymmetric "half-bulky" ligand precursor carrying a Me group and a *t*-Bu group on the two rings led directly to the  $\beta$ -abstraction product.

## Introduction

H-abstraction processes are fundamental steps in organometallic chemistry. Among these, the  $\alpha$ - and  $\beta$ -H abstractions are the most common, being the major pathways for the decomposition of metal-alkyl single bonds. In particular, the  $\alpha$ -H abstraction reaction, which leads to a metal-carbon double bond (along with alkane formation), has been extensively studied since its initial discovery in the early 1970s.<sup>1–3</sup> Studies concerning  $\alpha$ -H abstraction were performed mainly on group V (Ta) and group VI (Mo, W) metal complexes. Di- and trialkyl-metal complexes have been employed as the main substrates for the  $\alpha$ -H abstraction reaction, leading to the alkylidene and the alkyl-alkylidene complexes, respectively. The alkyl group should be free of  $\beta$ -hydrogens; otherwise, a competitive  $\beta$ -H elimination pathway becomes viable, resulting in the formation of a metal-olefin complex instead of the metal-alkylidene complex. Such basic studies are of major significance, since they may provide mechanistic insight and lead to the design of new ligand systems that may be ultimately employed in well-defined olefin metathesis catalysis.<sup>4,5</sup>

The use of predesigned ligand systems may offer a considerable advantage in this kind of study. Recently, we have been investigating the family of the amine bis(phenolate) ligands for group IV transition metals.<sup>6</sup> This family, comprised of dianionic [ONO] tridentate and [ONXO] tetradentate ligands, which differ from one another by the presence of an additional, so-called "side arm" donor, led to the formation of penta- and hexacoordinate complexes, respectively, with the [ONO] core donors in a *mer* arrangement and the two labile groups in a *cis* relationship. These complexes led to  $\alpha$ -olefin polymerization catalysts exhibiting a broad spectrum of activities. We found that the existence of the side-arm donor had a dramatic influence on the reactivity of these complexes. The Zr and Hf complexes of ligands with a side-arm donor were found to lead to highly active polymerization catalysts,<sup>6c,d</sup> while the corresponding Ti catalysts exhibited a prolonged living character.<sup>6a,b,e–g</sup> In contrast, the five-coordinate Zr

(4) Wallace, K. C.; Liu, A. H.; Dewan, J. C.; Schrock, R. R. *J. Am. Chem. Soc.* **1988**, *110*, 4964.

(5) For a recent review see: Fürstner, A. *Angew. Chem., Int. Ed.* **2000**, *39*, 3012.

(6) (a) Tshuva, E. Y.; Versano, M.; Goldberg, I.; Kol, M.; Weitman, H.; Goldschmidt, Z. *Inorg. Chem. Commun.* **1999**, *2*, 371. (b) Tshuva, E. Y.; Goldberg, I.; Kol, M.; Goldschmidt, Z. *Inorg. Chem. Commun.* **2000**, *3*, 611. (c) Tshuva, E. Y.; Goldberg, I.; Kol, M.; Goldschmidt, Z. *Organometallics* **2001**, *20*, 3017. (d) Tshuva, E. Y.; Groysman, S.; Goldberg, I.; Kol, M.; Goldschmidt, Z. *Organometallics* **2002**, *21*, 662. (e) Tshuva, E. Y.; Goldberg, I.; Kol, M.; Goldschmidt, Z. *Chem. Commun.* **2001**, 2120. (f) Groysman, S.; Goldberg, I.; Kol, M.; Genizi, E.; Goldschmidt, Z. *Inorg. Chim. Acta* **2003**, *345*, 137. (g) Groysman, S.; Goldberg, I.; Kol, M.; Goldschmidt, Z. *Organometallics* **2003**, *22*, 3013.

\* To whom correspondence should be addressed. E-mail: moshekol@post.tau.ac.il (M.K.); goldz@mail.biu.ac.il (Z.G.).

<sup>†</sup> Tel Aviv University.

<sup>‡</sup> Bar-Ilan University.

(1) Schrock, R. R. *Chem. Rev.* **2002**, *102*, 145 and references therein.

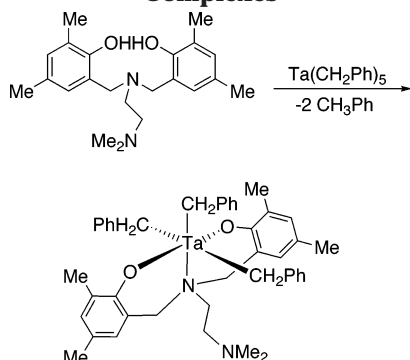
(2) (a) Schrock, R. R. *J. Organomet. Chem.* **1976**, *122*, 209. (b) Malatesta, V.; Ungold, K. U.; Schrock, R. R. *J. Organomet. Chem.* **1978**, *152*, C53. (c) Schrock, R. R. *Acc. Chem. Res.* **1979**, *12*, 98.

(3) Li, L.; Hung, M.; Xue, Z. *J. Am. Chem. Soc.* **1995**, *117*, 12746.

Table 1. Crystallographic Experimental Details

	3a	6a	2b	3b	5b	8b
formula	C <sub>39</sub> H <sub>45</sub> Cl <sub>4</sub> N <sub>2</sub> O <sub>2</sub> Ta· 1/2 C <sub>4</sub> H <sub>8</sub> O	C <sub>42</sub> H <sub>48</sub> NO <sub>2</sub> Ta	C <sub>29</sub> H <sub>62</sub> NO <sub>2</sub> Ta· C <sub>7</sub> H <sub>8</sub>	C <sub>32</sub> H <sub>31</sub> Cl <sub>4</sub> N <sub>2</sub> O <sub>2</sub> Ta· C <sub>7</sub> H <sub>8</sub>	C <sub>35</sub> H <sub>36</sub> NO <sub>3</sub> Ta· 1/2 C <sub>4</sub> H <sub>8</sub> O	C <sub>42</sub> H <sub>55</sub> N <sub>2</sub> O <sub>2</sub> Ta· C <sub>5</sub> H <sub>12</sub>
fw	932.57	779.76	743.89	890.47	737.67	872.98
a (Å)	11.6050(2)	12.1480(3)	8.2910(3)	10.9600(1)	15.8330(3)	14.0190(2)
b (Å)	13.2170(2)	12.5780(3)	13.0580(4)	14.1730(2)	10.6670(2)	17.1160(3)
c (Å)	14.6460(3)	23.2350(7)	17.2200(7)	23.5480(3)	19.8790(4)	17.7430(3)
α (deg)	114.999(1)	90.00	90.442(1)	90.00	90.00	90.00
β (deg)	98.716(1)	94.790(1)	98.517(1)	92.136(1)	100.676(1)	94.011(1)
γ (deg)	94.798(1)	90.00	94.348(3)	90.00	90.00	90.00
cryst syst	triclinic	monoclinic	triclinic	monoclinic	monoclinic	monoclinic
space group	P $\bar{1}$	P2 <sub>1</sub> /c	P $\bar{1}$	P2 <sub>1</sub> /n	P2 <sub>1</sub> /a	P2 <sub>1</sub> /n
V (Å <sup>3</sup> )	1984.95(6)	3537.85(16)	1838.10(11)	3655.31(8)	3299.26(11)	4246.99(12)
D <sub>c</sub> (g cm <sup>-3</sup> )	1.560	1.464	1.344	1.618	1.485	1.365
μ (cm <sup>-1</sup> )	3.077	3.143	3.021	3.336	3.369	2.626
Z	2	4	2	4	4	4
no. of measd rflns	9339	8310	8594	8745	7830	9887
no. of rflns with I > 2σ(I)	8189	4357	6092	7284	5389	7332
R1 (I > 2σ(I))	0.0395	0.0717	0.0737	0.0300	0.0434	0.0395
wR2 (I > 2σ(I))	0.0851	0.0828	0.1863	0.0662	0.0834	0.0851
GOF	1.015	0.963	1.051	1.048	0.999	1.015

## Scheme 1. Synthesis of Tribenzyltantalum Complexes



complexes featured fast deactivation, while the Ti catalysts lacking that donor led to oligomerization.<sup>6b,c</sup>

Furthermore, we demonstrated that the organometallic chemistry of the amine bis(phenolate) ligands is not limited to group IV metals.<sup>7a</sup> Our preliminary results have shown that Ta(CH<sub>2</sub>Ph)<sub>5</sub> undergoes a fast toluene elimination upon reaction with an [ONXO] amine bis(phenolate) ligand precursor at room temperature, affording an octahedral tribenzyl Ta(V) complex in which the side-arm donor was not bound to the metal (Scheme 1). Thus, at first sight, the role of a side-arm donor seemed much less evident in the Ta(V) chemistry. Having developed this straightforward synthesis to the tribenzyltantalum complexes, we turned to investigate their reactivity and, especially, evaluate the structural parameters (i.e. side-arm donor and phenolate ring substituents) that might favor the desired  $\alpha$ -abstraction path. Herein we describe these reactivity studies. We demonstrate that, in addition to the  $\alpha$ -abstraction route leading to benzyl–benzylidene complexes, there exists a competitive ligand backbone  $\beta$ -abstraction route. The structural parameters that promote each of these routes are discussed as well.

## Experimental Section

**General Considerations.** All manipulations of the metal complexes were performed under a dry nitrogen atmosphere

(7) (a) Groysman, S.; Goldberg, I.; Kol, M.; Goldschmidt, Z. *Organometallics* **2003**, *22*, 3793. (b) Groysman, S.; Segal, S.; Shamis, M.; Goldberg, I.; Kol, M.; Goldschmidt, Z.; Hayut-Salant, E. *J. Chem. Soc., Dalton Trans.* **2002**, 3425.

in a nitrogen-filled glovebox. Ta(CH<sub>2</sub>Ph)<sub>5</sub>,<sup>7a</sup> Lig<sup>1</sup>H<sub>2</sub>,<sup>6c</sup> Lig<sup>2</sup>H<sub>2</sub>,<sup>6a</sup> Lig<sup>4</sup>H<sub>2</sub>,<sup>6c</sup> and Lig<sup>6</sup>H<sub>2</sub>,<sup>6a</sup> were prepared according to previously published procedures. TaCl<sub>5</sub>, BnMgCl (1.0 M in ether), and hexamethyldisiloxane (98%) were obtained from Aldrich Inc. Ether and tetrahydrofuran were purified by reflux and distillation under a dry argon atmosphere from Na/benzophenone. Pentane was washed with HNO<sub>3</sub>/H<sub>2</sub>SO<sub>4</sub> prior to distillation from Na/benzophenone. Toluene was refluxed over molten Na and distilled under Ar. NMR data were collected on Bruker AC-200 and Bruker AC-400 spectrometers and referenced to protio impurities in benzene-*d*<sub>6</sub> ( $\delta$  7.15 ppm) and to the <sup>13</sup>C chemical shift of benzene ( $\delta$  128.70 ppm). Routine characterization of metal complexes consisted of <sup>1</sup>H, BB, and DEPT-135 <sup>13</sup>C NMR experiments, performed in C<sub>6</sub>D<sub>6</sub>. Kinetic data were obtained via variable-temperature (VT) <sup>1</sup>H NMR experiments, using hexamethyldisiloxane as an internal standard. VT NMR experiments for the decomposition of **2a** and **3a** were performed in C<sub>6</sub>D<sub>6</sub> (327 K). VT NMR experiments for the decomposition of **5a**, **6a**, and **7a** were performed in toluene-*d*<sub>8</sub> (338, 344, and 349 K). The uncertainty of the kinetic data is estimated to be 10%. X-ray diffraction measurements were performed on a Nonius Kappa CCD diffractometer system, using Mo K $\alpha$  ( $\lambda$  = 0.7107 Å) radiation. The analyzed crystals were embedded within a drop of viscous oil and freeze-cooled to ca. 110 K. The structures were solved by a combination of direct methods and Fourier techniques using DIRDIF software and were refined by full-matrix least squares with SHELXL-97. The crystal and experimental data are summarized in Table 1. Elemental analyses were performed in the microanalytical laboratory at the Hebrew University of Jerusalem. The analyzed complexes consistently showed a low carbon percentage due to their extreme air sensitivity.

**Preparation of the Amine Bis(phenolate) Ligands Lig<sup>3</sup>H<sub>2</sub>, Lig<sup>5</sup>H<sub>2</sub>, Lig<sup>7</sup>H<sub>2</sub>, Lig<sup>8</sup>H<sub>2</sub>.** Preparation of Lig<sup>5</sup>H<sub>2</sub>. A solution of 2,4-dichlorophenol (5.0 g, 30.7 mmol), 2-(dimethylamino)ethylamine (1.68 mL, 15.3 mmol), and 36% aqueous formaldehyde (3.6 mL, 43.2 mmol) in methanol (10 mL) was stirred and refluxed for 24 h. The mixture was cooled, and the product was filtered and washed with ice-cold methanol, to give the colorless product (3.4 g, 50.7%). Mp: 169 °C. Anal. Calcd for C<sub>18</sub>H<sub>20</sub>Cl<sub>4</sub>N<sub>2</sub>O<sub>2</sub>: C, 49.34; H, 4.60; Cl, 32.36; N, 6.39. Found: C, 49.34, H, 4.90; Cl, 32.06; N, 6.25. <sup>1</sup>H NMR (CDCl<sub>3</sub>, 200 MHz):  $\delta$  7.27 (d, *J* = 2.0 Hz, 2H), 6.92 (d, *J* = 2.0 Hz, 2H), 3.66 (s, 4H), 2.68 (m, 4H), 2.41 (s, 6H). <sup>13</sup>C NMR (CDCl<sub>3</sub>, 200 MHz):  $\delta$  151.7 (2C), 129.6 (2CH), 128.3 (2CH), 124.4 (2C), 123.5 (2C), 122.6 (2C), 56.0 (CH<sub>2</sub>), 55.7 (CH<sub>2</sub>), 49.1 (CH<sub>2</sub>), 44.8 (2CH<sub>3</sub>).

**Preparation of Lig<sup>5</sup>H<sub>2</sub>.** A solution of 2,4-dimethylphenol

(5.0 g, 40.9 mmol), 2-methoxyethylamine (1.78 mL, 20.5 mmol), and 36% aqueous formaldehyde (3.4 mL, 40.9 mmol) in methanol (10 mL) was stirred and refluxed for 24 h. The solution was cooled, and the product was filtered and washed with cold methanol (3 × 10 mL), affording colorless crystals (4.7 g, 67% yield). Mp: 22 °C. Anal. Calcd for C<sub>21</sub>H<sub>29</sub>NO<sub>3</sub>: C, 73.44; H, 8.51; N, 4.08. Found: C, 73.38; H, 8.51; N, 4.08. <sup>1</sup>H NMR (CDCl<sub>3</sub>, 200 MHz): δ 6.88 (d, *J* = 2.0 Hz, 2H), 6.68 (d, *J* = 2.0 Hz, 2H), 3.79 (s, 4H), 3.60 (t, *J* = 5.0 Hz, 2H), 3.47 (s, 3H), 2.77 (t, *J* = 5.0 Hz, 2H), 2.24 (s, 6H), 2.21 (s, 6H). <sup>13</sup>C NMR (CDCl<sub>3</sub>, 50.29 MHz): δ 152.2 (C), 131.4 (CH), 128.5 (CH), 128.1 (C), 125.3 (C), 120.7 (C), 71.1 (CH<sub>2</sub>), 59.1 (CH<sub>3</sub>), 57.1 (CH<sub>2</sub>), 51.0 (CH<sub>2</sub>), 20.4 (CH<sub>3</sub>), 16.1 (CH<sub>3</sub>).

**Preparation of Lig<sup>7</sup>H<sub>2</sub>.** A solution of 2,4-dichlorophenol (5.1 g, 30 mmol), 1-aminopropane (0.95 g, 15 mmol), and 36% aqueous formaldehyde (2.5 mL, 30 mmol) in methanol (10 mL) was stirred and refluxed for 22 h. After the mixture was cooled, the volatiles were removed under vacuum to give the crude product as a heavy brown oil that was purified first by column chromatography (silica gel, 5–10% ethyl acetate in hexane), followed by recrystallization from hexane to give the pure product as white crystals (2.3 g, 38% yield). Mp: 115–116 °C. Anal. Calcd for C<sub>17</sub>H<sub>17</sub>Cl<sub>2</sub>N<sub>2</sub>O<sub>2</sub>: C, 49.91; H, 4.19; N, 3.42. Found: C, 50.01; H, 4.36; N, 3.49. HRMS (DCI-I-Bu): 407.001 228 (C<sub>17</sub>H<sub>17</sub>Cl<sub>2</sub>N<sub>2</sub>O<sub>2</sub>; M<sup>+</sup>). <sup>1</sup>H NMR (CDCl<sub>3</sub>, 200 MHz): δ 7.26 (d, *J* = 2.0 Hz, 2H), 6.98 (d, *J* = 2.0 Hz, 2H), 5.90 (bs, 2H), 3.72 (s, 4H), 2.48 (m, 2H), 1.63 (m, 2H), 0.89 (t, *J* = 7.5 Hz, 3H). <sup>13</sup>C NMR (CDCl<sub>3</sub>, 50.29 MHz): δ 150.74 (C), 128.54 (CH), 128.48 (CH), 124.75 (C), 124.31 (C), 121.24 (C), 55.54, (CH<sub>2</sub>), 55.26 (2 CH<sub>2</sub>), 18.87 (CH<sub>2</sub>), 11.65 (CH<sub>3</sub>).

**Preparation of Lig<sup>8</sup>H<sub>2</sub>.** A solution of 2,4-dimethylphenol (1.83 g, 15.0 mmol), 2,4-di-*tert*-butylphenol (3.1 g, 15.0 mmol), 2-(dimethylamino)ethylamine (1.65 mL, 15.0 mmol), and 36% aqueous formaldehyde (3.5 mL, 42.0 mmol) in methanol (10 mL) was stirred and refluxed for 18 h. The mixture was cooled and decanted. TLC of the remaining solid (10% methanol–90% hexane) showed clearly the formation of three products: the two symmetric bis(phenols) and the cross-coupling product. A single crystallization of the mixture from methanol (100 mL) gave selectively the symmetrical 2,4-dimethyl derivative (2 g, mp 167 °C, 37% yield). The symmetrical 2,4-di-*tert*-butyl derivative (0.96 g, mp 130 °C, 13% yield) crystallized from the mother liquor. Finally, column chromatography (silica, chloroform) of the remaining mixture gave the pure crossed amine bis(phenol) as colorless crystals (1.86 g, 28.1% yield). Mp: 117 °C. Anal. Calcd for C<sub>28</sub>H<sub>44</sub>N<sub>2</sub>O<sub>2</sub>: C, 76.32; H, 10.06; N, 6.36. Found: C, 76.16, H, 10.24, N, 6.44. HRMS: calcd, 441.348 10 (MH<sup>+</sup>); found, 441.350 00. <sup>1</sup>H NMR (CDCl<sub>3</sub>, 200 MHz): δ 7.18 (d, *J* = 2.0 Hz, 2H), 6.85 (d, *J* = 2.0 Hz, 2H), 6.85 (s, 1H), 6.68 (s, 1H), 3.64 (s, 2H), 3.56 (s, 2H), 2.58 (s, 4H), 2.32 (s, 6H), 2.19 (s, 6H), 1.38 (s, 9H), 1.36 (s, 9H). <sup>13</sup>C NMR (CDCl<sub>3</sub>, 200 MHz): δ 153.2 (C), 152.7 (C), 140.4 (C), 135.9 (C), 131.1 (CH), 128.6 (CH), 127.3 (C), 125.6 (C), 124.6 (CH), 123.3 (CH), 121.6 (C), 57.3 (CH<sub>2</sub>), 56.1 (CH<sub>2</sub>), 55.2 (CH<sub>2</sub>), 48.9 (CH<sub>2</sub>), 44.9 (CH<sub>3</sub>), 35.0 (C), 34.1 (C), 31.7 (CH<sub>3</sub>), 29.6 (CH<sub>3</sub>), 20.3 (CH<sub>3</sub>), 16.2 (CH<sub>3</sub>).

**Preparation of the Tribenzyl Complexes 2a–7a. General Procedure.** Lig<sup>2</sup>H<sub>2</sub>–Lig<sup>7</sup>H<sub>2</sub> were dissolved in ca. 1 mL of toluene and added dropwise to a stirred red-brown solution of Ta(CH<sub>2</sub>Ph)<sub>5</sub> (1 equiv) in ca. 1 mL of toluene. The resulting dark yellow solution was stirred at room temperature. After 2 h the solvent was removed in vacuo, leading to the yellow-orange 2a–7a quantitatively.

**2a.** <sup>1</sup>H NMR (C<sub>6</sub>D<sub>6</sub>, 298 K, 200 MHz): δ 7.21 (d, *J* = 7.4 Hz, 6H), 7.07 (t, *J* = 7.4 Hz, 6H), 6.80 (m, 5H), 6.64 (s, 2H), 3.84 (d, *J* = 13.9 Hz, 2H), 3.35 (d, *J* = 13.9 Hz, 2H), ca. 3.3 (br s, 6H), 1.99 (s, 12H), 1.76 (t, *J* = 5.8 Hz, 2H), 1.62 (s, 6H), 1.54 (t, *J* = 6.0 Hz, 2H); <sup>13</sup>C NMR (C<sub>6</sub>D<sub>6</sub>, 298 K, 50.29 MHz): δ 156.92 (C), 132.11 (CH), 131.49 (CH), 131.05 (CH), 128.97

(CH), 128.43 (CH), 128.35 (CH), 119.82 (CH), 122.66 (C), 57.16 (CH<sub>2</sub>), 53.62 (CH<sub>2</sub>), 46.57 (CH<sub>3</sub>), 44.06 (CH<sub>2</sub>), 20.32 (CH<sub>3</sub>), 19.59 (CH<sub>3</sub>).

**3a.** Anal. Calcd for C<sub>39</sub>H<sub>39</sub>Cl<sub>4</sub>N<sub>2</sub>O<sub>2</sub>Ta: C, 52.60; H, 4.41; N, 3.15. Found: C, 51.39; H, 4.60; N, 3.21. <sup>1</sup>H NMR (C<sub>6</sub>D<sub>6</sub>, 298 K, 200 MHz): δ 7.19 (d, *J* = 2.3 Hz, 2H), 7.11, 7.02 (two overlapping br s, 12 H), 6.75 (br s, 3H), 6.63 (d, *J* = 2.3 Hz, 2H), 3.59 (d, *J* = 14.1, 2H), 3.31 (br s, 6H), 3.03 (d, *J* = 14.2, 2H), 1.46 (s, 6H), 1.36 (m, 3H), 1.04 (m, 2H). <sup>1</sup>H NMR (C<sub>6</sub>D<sub>6</sub>, 323 K, 200 MHz): δ 7.23 (d, *J* = 2.5 Hz, 2H), 7.11 (d, *J* = 7.4 Hz, 6H), 7.00 (t, *J* = 7.4 Hz, 2H), 6.74 (t, *J* = 7.2, 3H), 6.63 (d, *J* = 2.5 Hz, 2H), 3.56 (d, *J* = 14.2 Hz, 2H), 3.30 (s, 6H), 3.07 (d, *J* = 14.1 Hz, 2H), 1.49 (s, 6H), 1.45 (m, 2H), 1.14 (m, 2H). <sup>13</sup>C NMR (C<sub>6</sub>D<sub>6</sub>, 298 K, 50.29 MHz): δ 153.34 (C), 130.89 (CH), 129.89 (CH), 128.98 (CH), 131.96 (C), 127.70 (C), 127.61 (C), 125.03 (CH), 124.75 (C), ca. 85 (br s, CH<sub>2</sub>), 56.58 (CH<sub>2</sub>), 53.98 (CH<sub>2</sub>), 46.22 (CH<sub>3</sub>), 43.74 (CH<sub>2</sub>).

**4a.** The preparation and NMR characterization were reported previously.<sup>7a</sup> Anal. Calcd for C<sub>43</sub>H<sub>51</sub>N<sub>2</sub>O<sub>2</sub>Ta: C, 63.86; H, 6.36; N, 3.46. Found: C, 64.20; H, 6.44; N, 3.39.

**5a.** <sup>1</sup>H NMR (C<sub>6</sub>D<sub>6</sub>, 298 K, 200 MHz): δ 7.15–6.97 (Ar H, 12H), 6.85 (d, *J* = 1.5 Hz, 2H), 6.78 (br s, 3H), 6.57 (d, *J* = 1.8 Hz, 2H), 3.82 (d, *J* = 13.5, 2H), 3.42 (d, *J* = 13.6 Hz, 2H), 3.3 (br s, 4H), 3.09 (br s, 2H), 2.83 (t, *J* = 4.7 Hz, 2H), 2.71 (s, 3H), 2.29 (s, 6H), 2.12 (s, 6H), 1.66 (t, *J* = 5.0 Hz, 2H). <sup>1</sup>H NMR (C<sub>6</sub>D<sub>6</sub>, 323 K, 200 MHz): δ 7.11–6.97 (Ar H, 12H), 6.88 (d, *J* = 1.1 Hz, 2H), 6.76 (t, *J* = 6.9 Hz, 3H), 6.57 (d, *J* = 1.3 Hz, 2H), 3.78 (d, *J* = 13.7 Hz, 2H), 3.42 (d, *J* = 13.8 Hz, 2H), 3.19 (s, 6H), 2.88 (t, *J* = 5.0 Hz, 2H), 2.73 (s, 3H), 2.29 (s, 6H), 2.12 (s, 6H), 1.72 (t, *J* = 5.0 Hz, 2H). <sup>13</sup>C NMR (C<sub>6</sub>D<sub>6</sub>, 298 K, 50.29 MHz): δ 155.17 (C), 132.73 (CH), 132.25 (CH), 131.37 (CH), 129.97 (C), 129.57 (CH), 128.99 (CH), 128.59 (CH), 127.16 (C), 125.06 (C), ca. 80 (br s), 69.09 (CH<sub>2</sub>), 59.04 (CH<sub>3</sub>), 58.03 (CH<sub>2</sub>), 45.74 (CH<sub>2</sub>), 21.43 (CH<sub>3</sub>), 16.89 (CH<sub>3</sub>).

**6a.** <sup>1</sup>H NMR (C<sub>6</sub>D<sub>6</sub>, 298 K, 200 MHz) δ 7.23–6.56 (Ar H, 19H), 3.81 (d, *J* = 14.0, 2H), 3.39 (br s, 4H), ca. 3.0 (br s, 2H), 2.96 (d, *J* = 14.1, 2H), 1.96 (s, 12H), 1.35 (m, 2H), 0.86 (m, 2H), 0.03 (t, *J* = 7.2 Hz, 3H). <sup>13</sup>C NMR (C<sub>6</sub>D<sub>6</sub>, 298 K, 50.29 MHz): δ 157.02 (C), 139.19 (C), 131.55 (C), 131.50 (CH), 131.38 (C), 131.22 (CH), 128.47 (CH), 124.51 (CH), 122.45 (C), 119.92 (CH), 80.0 (br s, CH<sub>2</sub>), 56.37 (CH<sub>2</sub>), 48.96 (CH<sub>2</sub>), 20.38 (CH<sub>3</sub>), 19.68 (CH<sub>3</sub>), 11.86 (CH<sub>2</sub>), 11.33 (CH<sub>3</sub>).

**7a.** <sup>1</sup>H NMR (C<sub>6</sub>D<sub>6</sub>, 298 K, 200 MHz): δ 7.18 (d, *J* = 2.5 Hz, 2H), 7.10, 7.02, and 6.76 (3 overlapping br s, 15 H), 6.51 (d, *J* = 2.4, 2H), 3.45 and ca. 3.4 (overlapping peaks: d, *J* = 14.3 Hz, and br s, 8H), 2.52 (d, *J* = 14.3 Hz, 2H), 0.96 (m, 2H), 0.45 (m, 2H), –0.13 (t, *J* = 7.2 Hz, 3H). <sup>13</sup>C NMR (C<sub>6</sub>D<sub>6</sub>, 298 K, 100.62 MHz): δ 153.60 (C), 131.23 (CH), 129.98 (C), 129.117 (C), 128.66 (CH), 128.54 (CH), 127.92 (C), 127.26 (CH), 126.34 (C), 125.31 (CH), 124.99 (C), 55.61 (CH<sub>2</sub>), 49.03 (CH<sub>2</sub>), 11.82 (CH<sub>2</sub>), 10.95 (CH<sub>3</sub>).

**Preparation and Characterization of the Benzyl–Benzylidene (2b, 3b) and Dibenzyl Complexes (5b–8b).**

**Preparation of 2b.** 2a (207 mg, 0.256 mmol) was dissolved in toluene (4 mL) and was heated to 85 °C for 1 h. The reaction mixture was cooled, and the solvent was removed in vacuo, leading to a yellow-orange crude product. <sup>1</sup>H NMR of the crude product indicated the formation of an essentially pure mixture of two alkyl–alkylidene products in an approximately 3:1 ratio, as revealed from the Ta=C(Ph)H peaks at 9.28 and 9.17 ppm and the Ta–CH<sub>2</sub>Ph peaks at 2.94 and 2.89 ppm. The major product (2b) is obtained upon crystallization from cold ether in 22% yield (20 mg of 2b from 90 mg of the crude mixture). <sup>1</sup>H NMR (C<sub>6</sub>D<sub>6</sub>, 298 K, 200 MHz): δ 9.17 (s, 1H, Ta=C(Ph)H), 7.50 (m, 4H), 7.28 (d, *J* = 8.0 Hz, 2H), 7.11 (t, *J* = 7.8 Hz, 2H), 6.79 (m, 4H), 6.62 (s, 2H), 4.13 (d, *J* = 13.6 Hz, 2H), 2.94 (s, 2H), 2.67 (d, *J* = 13.6 Hz, 2H), 2.05 (s, 6H), 1.97 (s, 6H), 1.94 (br s, 8H), 1.37 (m, 2H). <sup>13</sup>C NMR (C<sub>6</sub>D<sub>6</sub>, 298 K, 50.29 MHz): δ 247.25 (Ta=C(Ph)H), 157.53 (C), 154.41 (C), 146.97 (C), 139.14 (C), 132.03 (CH), 130.03 (CH), 129.48 (C), 128.80 (CH), 127.85 (CH), 125.25 (CH), 123.85 (C), 121.48 (CH),

120.39 (CH), 64.72 (CH<sub>2</sub>), 63.25 (CH<sub>2</sub>), 60.49 (CH<sub>2</sub>), 53.07 (CH<sub>2</sub>), 50.69 (N(CH<sub>3</sub>)<sub>2</sub>), 20.30 (Ar-CH<sub>3</sub>), 19.60 (Ar-CH<sub>3</sub>).

**Formation of the Alkyl-Alkylidene 3b/3c Mixture upon 3a Decomposition.** A 15 mg portion of **3a** was dissolved in ca. 0.5 mL of C<sub>6</sub>D<sub>6</sub> and the solution heated to 80 °C for 1 h in an NMR tube. According to the <sup>1</sup>H NMR spectrum, the resulting crude product consists of an essentially pure mixture of the two alkyl-alkylidene products **3b** and **3c** in a ca. 1.5:1 ratio (C<sub>6</sub>D<sub>6</sub>, δ, selected absorptions): 8.95 and 8.80 ppm for Ta=C(Ph)H, 2.93 and 2.91 ppm for Ta-CH<sub>2</sub>Ph, 1.86 and 1.68 ppm for N(CH<sub>3</sub>)<sub>2</sub>.

**Large-Scale Preparation of 3b.** A 397 mg portion (0.45 mmol) of **3a** was dissolved in 7 mL of toluene and the solution heated for 1 h to 85–90 °C. After the concentration of the solvent to ca. 3 mL, the crude mixture was left in the glovebox freezer (–35 °C). Four crops (143 mg) of red-orange crystals were collected, giving pure **3b** in 44% yield. Anal. Calcd for C<sub>32</sub>H<sub>31</sub>Cl<sub>4</sub>N<sub>2</sub>O<sub>2</sub>Ta·C<sub>7</sub>H<sub>8</sub>: C, 52.60; H, 4.41; N, 3.15. Found: C, 51.12; H, 4.26; N, 3.43. <sup>1</sup>H NMR (C<sub>6</sub>D<sub>6</sub>, 298 K, 200 MHz): δ 8.81 (s, 1H), 7.46 (d, *J* = 7.3 Hz, 2H), 7.37 (t, *J* = 7.3 Hz, 2H), 7.19 (d, *J* = 2.5 Hz, 2H), 7.07 (d, *J* = 1.6 Hz, 2H), 7.05 (s, 2H), 6.76 (m, 2H), 6.55 (d, *J* = 2.5 Hz, 2H), 3.71 (d, *J* = 13.9 Hz, 2H), 2.91 (s, 2H), 2.21 (d, *J* = 14.0 Hz, 2H), 1.86 (s, 6H), 1.48 (m, 2H), 1.14 (m, 2H). <sup>13</sup>C NMR (C<sub>6</sub>D<sub>6</sub>, 298 K, 50.29 MHz): δ 249.31 (Ta=C(Ph)H, <sup>1</sup>J<sub>C-H</sub> = 106 Hz), 153.99 (C), 153.22 (C), 145.69 (C), 131.82 (CH), 131.22 (CH), 129.97 (C), 129.29 (CH), 128.99 (C), 128.53 (CH), 128.39 (CH), 127.42 (CH), 126.56 (CH), 126.34 (C), 126.12 (C), 125.32 (C), 122.01 (CH), 65.87 (CH<sub>2</sub>), 62.40 (CH<sub>2</sub>), 60.12 (CH<sub>2</sub>), 52.81 (CH<sub>2</sub>), 50.46 (CH<sub>3</sub>).

**Preparation and Characterization of 5b.** **5a** (73 mg, 0.10 mmol) in toluene (3 mL) was heated to 80 °C for 1 h. The solvent was removed in vacuo, leading to a yellow-orange crude product. A 53 mg amount of the crude mixture was extracted with ca. 2 mL of ether and kept at –35 °C for several days, giving pure **5b** as yellow crystals (18 mg, 34%). <sup>1</sup>H NMR (C<sub>6</sub>D<sub>6</sub>, 298 K, 200 MHz): δ 7.57 (d, *J* = 7.1 Hz, 2H), 7.38 (t, *J* = 7.4 Hz, 2H), 7.02 (m, 3H), 6.88 (d, *J* = 8.1 Hz, 2H), 7.70 (m, 3H), 6.61 (d, *J* = 2.1 Hz, 1H), 6.25 (d, *J* = 2.0 Hz, 1H), 3.50 (d, *J* = 14.4 Hz, 1H), 3.49 (s, 1H), 3.38 (d, *J* = 11.9 Hz, 1H), 3.28 (d, *J* = 11.1 Hz, 1H), 3.18 (d, *J* = 14.4 Hz, 1H), ca. 3.0 (m, 2H), 2.94 (d, *J* = 11.9 Hz, 1H), 2.65 (d, *J* = 11.2 Hz, 1H), 2.57 (s, 3H), 2.36 (m, 2H), 2.30 (s, 3H), 2.26 (s, 3H), 2.20 (s, 3H), 2.06 (s, 3H). <sup>13</sup>C NMR (C<sub>6</sub>D<sub>6</sub>, 298 K, 50.29 MHz): δ 150.13 (C), 149.75 (C), 132.40 (CH), 131.74 (CH), 130.86 (C), 129.98 (CH), 129.50 (C), 129.40 (CH), 129.01 (CH), 128.86 (CH), 128.52 (C), 128.44 (CH), 128.36 (C), 126.53 (CH), 126.36 (C), 126.22 (C), 125.19 (C), 123.68 (C), 123.24 (CH), 123.11 (CH), 81.89 (CH), 76.28 (CH<sub>2</sub>), 75.72 (CH<sub>2</sub>), 63.54 (CH<sub>2</sub>), 59.46 (CH<sub>3</sub>), 51.43 (CH<sub>2</sub>), 21.51 (CH<sub>3</sub>), 21.22 (CH<sub>3</sub>), 16.89 (CH<sub>3</sub>), 16.70 (CH<sub>3</sub>).

**Preparation of 6b (One Pot, from Lig<sup>6</sup>H<sub>2</sub> and Ta(CH<sub>2</sub>Ph)<sub>5</sub>).** A 37 mg amount (0.11 mmol) of Lig<sup>6</sup>H<sub>2</sub> in ca. 1 mL of toluene was added dropwise to a red-brown solution of Ta(CH<sub>2</sub>Ph)<sub>5</sub> (72 mg, 0.11 mmol) in ca. 1 mL of toluene. After it was stirred for 2 h at room temperature, the reaction mixture was heated to 90 °C for an additional 2 h. The solvent was removed in vacuo, and the crude product was extracted with ca. 4 mL of pentane. Cooling to –35 °C for 1 h and filtering off the solid impurities led to a bright yellow pentane solution. Solvent removal yielded 35 mg (0.05 mmol, 46% yield) of **6b** as a bright yellow solid. <sup>1</sup>H NMR + COSY + HMQC (C<sub>6</sub>D<sub>6</sub>, 298 K, 400 MHz): δ 7.43 (d, *J* = 7.7 Hz, 2H), 7.28 (t, *J* = 7.7 Hz, 2H), 7.05 (t, 7.3, 1H), 6.94 (d, *J* = 7.9 Hz, 2H), 6.85 (t, 7.8 Hz, 2H), 6.57 (m, 2H), 6.36 (s, 1H), 6.33 (s, 1H), 6.32 (s, 1H), 3.92 (d, *J* = 13.7 Hz, 1H), 3.82 (d, *J* = 13.8 Hz, 1H), 3.31 (d, *J* = 11.9 Hz, 1H), 3.16 (d, *J* = 12.0 Hz, 1H), 2.75 (s, 1H, PhCH(N)Ta), 2.69 (m, 2H, NCH<sub>2</sub>CH<sub>2</sub>CH<sub>3</sub>), 2.60 (d, *J* = 11.1 Hz, 1H), 2.48 (d, *J* = 11.1 Hz, 1H), 1.99 (s, 3H, Ar-CH<sub>3</sub>), 1.94 (s, 3H, Ar-CH<sub>3</sub>), 1.92 (s, 3H, Ar-CH<sub>3</sub>), 1.88 (s, 3H, Ar-CH<sub>3</sub>), 1.43 (m, 1H, NCH<sub>2</sub>CH<sub>2</sub>CH<sub>3</sub>), 1.03 (m, 1H, NCH<sub>2</sub>CH<sub>2</sub>CH<sub>3</sub>), 0.29 (t, *J* = 7.4 Hz, 3H, NCH<sub>2</sub>CH<sub>2</sub>CH<sub>3</sub>). <sup>13</sup>C NMR (C<sub>6</sub>D<sub>6</sub>, 298 K, 50.29 MHz): δ 158.50 (C), 144.17 (C), 136.61 (C), 136.23 (C),

133.92 (CH), 131.77 (CH), 131.50 (CH), 131.43 (CH), 130.01 (C), 129.42 (C), 129.00 (C), 128.48 (C), 125.48 (CH), 123.84 (CH), 123.01 (C), 119.34 (CH), 115.81 (CH), 80.81 (CH), 74.23 (CH<sub>2</sub>), 62.40 (CH<sub>2</sub>), 56.25 (CH<sub>2</sub>), 54.64 (CH<sub>2</sub>), 20.55 (CH<sub>3</sub>), 20.33 (CH<sub>3</sub>), 20.13 (CH<sub>2</sub>), 19.74 (CH<sub>3</sub>), 19.60 (CH<sub>3</sub>), 12.51 (CH<sub>3</sub>).

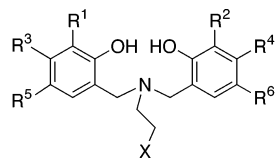
**Preparation of 7b.** A 91 mg amount (0.105 mmol) of **7a** in 4 mL of toluene was heated to ca. 90 °C for 4.5 h. The reaction was monitored by <sup>1</sup>H NMR spectroscopy, which indicated that **7b** was the only organometallic (diamagnetic) product formed. After toluene removal, the resulting yellow-brown solid was extracted with ca. 3 mL of diethyl ether. Cooling in the glovebox freezer (–35 °C) for 24 h yielded yellow microcrystals of **7b** (11 mg, 0.014 mmol, 14% yield). Subsequent workup of the ether solution, which was comprised of ether evaporation and pentane washings, yielded another 27 mg of essentially pure **7b**. <sup>1</sup>H NMR (C<sub>6</sub>D<sub>6</sub>, 298 K, 200 MHz): δ 7.17 (m, 2H), 7.02 (d, *J* = 7.3 Hz, 4H), 6.91 (t, *J* = 7.7 Hz, 4H), 6.76 (t, *J* = 7.2 Hz, 2H), 6.47 (d, *J* = 2.5 Hz, 1H), 6.42 (d, *J* = 2.3 Hz, 1H), 3.43 (AB system, *J* = 14.4 Hz, 2H), 2.50 (m, 5H), 2.36 (m, 2H), 1.10 (m, 1H), 0.80 (m, 1H), 0.19 (t, *J* = 7.4 Hz, 3H). <sup>13</sup>C NMR + DEPT-135 (C<sub>6</sub>D<sub>6</sub>, 298 K, 50.29 MHz): δ 132.97 (CH), 131.11 (CH), 130.87 (CH), 130.46 (CH), 130.22 (CH), 129.98 (C), 129.89 (CH), 129.12 (CH), 129.02 (CH), 128.88 (C), 128.39 (C), 127.80 (CH), 126.88 (CH), 126.35 (C), 125.69 (CH), 77.05 (CH), 71.81 (CH<sub>2</sub>), 64.75 (CH<sub>2</sub>), 56.25 (CH<sub>2</sub>), 55.03 (CH<sub>2</sub>), 20.09 (CH<sub>2</sub>), 12.25 (CH<sub>3</sub>).

**Preparation of 8b.** A 58 mg portion (0.13 mmol) of Lig<sup>8</sup>H<sub>2</sub> was dissolved in ca. 1 mL of toluene and slowly added to a red-brown solution of Ta(CH<sub>2</sub>Ph)<sub>5</sub> (86 mg, 0.13 mmol) in ca. 1 mL of toluene. The resulting mixture was stirred for 2 h at room temperature, after which the solvent was removed in vacuo. The crude **8b** was washed once with pentane (3 mL), leading to 52 mg (0.065 mmol, 50% yield) of pure **8b**. X-ray-quality crystals were obtained from cold (–35 °C) ether. <sup>1</sup>H NMR (C<sub>6</sub>D<sub>6</sub>, 298 K, 200 MHz): δ 7.57 (d, *J* = 7.7 Hz, 2H), 7.40 (t, *J* = 7.8 Hz, 2H), 7.33 (d, *J* = 2.2 Hz, 1H), 6.98 (m, 4 H), 6.67 (m, 4H), 6.23 (br s, 1H), 3.61 (d, *J* = 14.8 Hz, 1H), 3.29 (m, 2H), 3.24 (d, *J* = 15.1 Hz, 1H), 2.71 and 2.82 (overlapping AB system and m, *J* = 11.6 Hz for the AB system, 3H), 2.41 (m, 1H), 2.13 (s, 3H, Ar-CH<sub>3</sub>), 2.06 (s, 3H, Ar-CH<sub>3</sub>), 2.00 (s, 6H, N(CH<sub>3</sub>)<sub>2</sub>), 1.53 (s, 9H, Ar-C(CH<sub>3</sub>)<sub>3</sub>), 1.39 (s, 9H, Ar-C(CH<sub>3</sub>)<sub>3</sub>). <sup>13</sup>C NMR (C<sub>6</sub>D<sub>6</sub>, 298 K, 50.29 MHz): δ 161.51 (C), 154.95 (C), 153.01 (C), 142.32 (C), 135.32 (C), 135.05 (CH), 132.56 (CH), 131.06 (C), 129.01 (C), 128.94 (CH), 128.59 (CH), 127.99 (CH), 127.79 (C), 127.68 (CH), 125.96 (CH), 123.55 (CH), 122.58 (CH), 121.89 (CH), 110.09 (Ta-CH), 76.27 (CH<sub>2</sub>), 75.85 (CH<sub>2</sub>), 64.82 (CH<sub>2</sub>), 64.63 (CH<sub>2</sub>), 53.79 (CH<sub>2</sub>), 50.10 (CH<sub>3</sub>), 35.27 (C), 32.80 (CH<sub>3</sub>), 32.71 (C), 31.49 (CH<sub>3</sub>), 21.29 (CH<sub>3</sub>), 16.99 (CH<sub>3</sub>).

**Kinetic Experiments. <sup>1</sup>H NMR Monitoring of 2a Decomposition.** A 27 mg portion (0.033 mmol) of **2a** was dissolved in benzene-*d*<sub>6</sub> (containing hexamethyldisiloxane). The final volume of the solution was 0.40 mL. The resulting solution was heated to 327(1) K in the NMR probe for 140 min, being sampled (by <sup>1</sup>H NMR) every 10 min.

**<sup>1</sup>H NMR Monitoring of 3a Decomposition.** A 17 mg portion (0.074 mmol) of **3a** was dissolved in benzene-*d*<sub>6</sub> (0.60 mL total volume), resulting in a 0.123 M **3a** solution. The resulting solution was heated to 327(1) K in the NMR probe for 180 min, being sampled (by <sup>1</sup>H NMR) every 5 min.

**<sup>1</sup>H NMR Monitoring of 5a Decomposition.** Since no decomposition of **5a** was observed at 327(1) K in benzene-*d*<sub>6</sub> (for 40 min), higher temperature experiments were attempted. A 15 mg portion (0.019 mmol) of **5a** in toluene-*d*<sub>8</sub> (0.40 mL, 0.047 M) was reacted at 338(1) K for 240 min, with sampling every 10 min. A 17 mg portion (0.021 mmol) in toluene-*d*<sub>8</sub> (0.38 mL, 0.055 M) was heated to 344(1) K for 180 min (until **5a** reached ca. 1/10 of its initial concentration), with sampling every 10 min. A 17 mg portion (0.021 mmol) of **5a** (0.40 mL, 0.053 M) was heated to 349(1) K for 120 min, with sampling every 5 min.



Lig<sup>1</sup>H<sub>2</sub>: R<sup>1</sup>=R<sup>2</sup>=R<sup>5</sup>=R<sup>6</sup>=*t*-Bu, R<sup>3</sup>=R<sup>4</sup>=H, X=NMe<sub>2</sub>

Lig<sup>2</sup>H<sub>2</sub>: R<sup>1</sup>=R<sup>2</sup>=H, R<sup>3</sup>=R<sup>4</sup>=R<sup>5</sup>=R<sup>6</sup>=Me, X=NMe<sub>2</sub>

Lig<sup>3</sup>H<sub>2</sub>: R<sup>1</sup>=R<sup>2</sup>=R<sup>5</sup>=R<sup>6</sup>=Cl, R<sup>3</sup>=R<sup>4</sup>=H, X=NMe<sub>2</sub>

Lig<sup>4</sup>H<sub>2</sub>: R<sup>1</sup>=R<sup>2</sup>=R<sup>5</sup>=R<sup>6</sup>=Me, R<sup>3</sup>=R<sup>4</sup>=H, X=NMe<sub>2</sub>

Lig<sup>5</sup>H<sub>2</sub>: R<sup>1</sup>=R<sup>2</sup>=R<sup>5</sup>=R<sup>6</sup>=Me, R<sup>3</sup>=R<sup>4</sup>=Me, X=OMe

Lig<sup>6</sup>H<sub>2</sub>: R<sup>1</sup>=R<sup>2</sup>=H, R<sup>3</sup>=R<sup>4</sup>=R<sup>5</sup>=R<sup>6</sup>=Me, X=Me

Lig<sup>7</sup>H<sub>2</sub>: R<sup>1</sup>=R<sup>2</sup>=R<sup>5</sup>=R<sup>6</sup>=Cl, R<sup>3</sup>=R<sup>4</sup>=H, X=Me

Lig<sup>8</sup>H<sub>2</sub>: R<sup>1</sup>=R<sup>5</sup>=Me, R<sup>2</sup>=R<sup>6</sup>=*t*-Bu, R<sup>3</sup>=R<sup>4</sup>=H, X=NMe<sub>2</sub>

**Figure 1.** Amine bis(phenolate) ligands employed in this study.

**6a/7a Decomposition Experiments.** The kinetic experiment monitoring **6a** decomposition was performed at 349(1) K. A 20 mg portion (0.026 mmol) of **6a** in toluene-*d*<sub>8</sub> (0.44 mL, 0.059 M) was heated to the desired temperature for 180 min, being sampled by <sup>1</sup>H NMR every 10 min. When **7a** was heated to the same (349(1) K) temperature, no sign of decomposition was detected for at least 50 min.

## Results and Discussion

The amine bis(phenolate) ligands employed in this study are presented in Figure 1. Lig<sup>1</sup>H<sub>2</sub>–Lig<sup>4</sup>H<sub>2</sub> are all [ONNO]-type ligands bearing a dimethylamino donor on a side arm and differ in their phenolate substituents. Lig<sup>1</sup>H<sub>2</sub> is the bulkiest, featuring *tert*-butyl groups in the ortho positions of the phenolate oxygens, whereas Lig<sup>2</sup>H<sub>2</sub> is the least bulky, featuring H atoms in ortho positions. Lig<sup>3</sup>H<sub>2</sub> features electron-withdrawing chloro groups, and Lig<sup>4</sup>H<sub>2</sub> has an intermediate steric bulk featuring *o*-methyl substituents. Lig<sup>5</sup>H<sub>2</sub> is analogous to Lig<sup>4</sup>H<sub>2</sub>, except for having a methoxy side-arm donor. In contrast, the [ONO]-type Lig<sup>6</sup>H<sub>2</sub> and Lig<sup>7</sup>H<sub>2</sub> have no side-arm donor. Finally, the reactivity of the “half-bulky” Lig<sup>8</sup>H<sub>2</sub>, bearing different substituents (*t*-Bu and Me) on the phenolate rings (Figure 1), toward Ta(CH<sub>2</sub>Ph)<sub>5</sub> was investigated. All ligands were prepared by a single-step Mannich condensation among the suitable phenol, amine, and formaldehyde, as previously described,<sup>6</sup> except for the asymmetric Lig<sup>8</sup>H<sub>2</sub>, which was synthesized from a mixture of two different phenols and was purified by consecutive crystallizations and chromatography.

In contrast to their reaction with group IV tetrabenzyl complexes, the reaction of the ligand precursors with Ta(CH<sub>2</sub>Ph)<sub>5</sub> was found to depend strongly on the bulk of the aromatic ring substituents: the ligand bearing *t*-Bu groups in the ortho position of both phenolates (Lig<sup>1</sup>H<sub>2</sub>) did not show any appreciable reactivity toward pentabenzyltantalum precursor at room temperature for hours. On the other hand, the ligand precursors Lig<sup>2</sup>H<sub>2</sub>–Lig<sup>7</sup>H<sub>2</sub> reacted with pentabenzyltantalum at room temperature, giving the tribenzyl complexes **2a**–**7a** in high yields. Complexes **2a**–**7a** exhibit a somewhat dual character in solution at room temperature: The amine bis(phenolate) ligand-to-metal binding is rigid, according to the AB pattern of the ligand methylene protons and

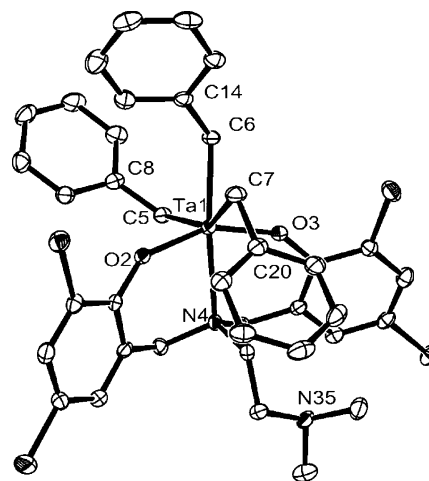


**Figure 2.** ORTEP drawing of **3a** (50% probability ellipsoids). The hydrogen atoms and the crystallization solvent were omitted for clarity. Selected bond distances (Å) and angles (deg): Ta1–O2 = 1.916(2), Ta1–O3 = 1.895(2), Ta1–N4 = 2.506(3), Ta1–C5 = 2.224(4), Ta1–C6 = 2.267(3), Ta1–C7 = 2.246(3); O3–Ta1–O2 153.12(10), C6–Ta1–N4 = 158.29(11), C5–Ta1–C7 = 148.30(12).

to the overall *C*<sub>s</sub> symmetry on the NMR time scale, whereas the benzyl ligands are highly fluxional at room temperature, giving rise to two broad signals in the aliphatic region. Slight heating (to ca. 40 °C) of **2a**–**7a** coalesces the benzyl signals into one broad singlet, while cooling to ca. –50 °C (measured for **4a**) resolves three distinct benzyl systems, as expected for a *C*<sub>s</sub>-symmetrical complex having three different benzyl groups lying on a mirror plane. The identical behavior of **2a**–**7a** in solution at or near room temperature implies that the side-arm donor, present in complexes **2a**–**5a**, is not coordinating to the metal center in solution. To gain further structural information regarding these types of compounds, we carried out X-ray structure determinations for **3a**, **4a**, and **6a** (Figures 2–4, respectively). As expected, the Ta(V) metal in all three structures is hexacoordinate, with the side-arm donor unbound. The geometry around the metal may be defined as distorted octahedral. The tridentate [ONO] cores of the ligands bind to the metal in a *mer* fashion, resulting in a *mer* disposition of the three benzyl groups. The Ta–O bond lengths lie in the relatively narrow range of 1.876(3)–1.916(2) Å and closely resemble those normally observed for early-transition-metal phenolate complexes.<sup>4,6–10</sup> The nitrogen-to-metal bond lengths in all three structures are longer than previously observed for related group IV complexes (2.506(3)–2.548(6) Å).<sup>6,11</sup> This trend may be attributed to the presence of the three electron-

(8) Kim, Y.; Kapoor, P. N.; Verkade, J. G. *Inorg. Chem.* **2002**, *41*, 4834.

(9) (a) Chamberlain, L. R.; Rothwell, I. P.; Folting, K.; Huffman, J. C. *J. Chem. Soc., Dalton Trans.* **1987**, 155. (b) Vilardo, J. S.; Lockwood, M. A.; Hanson, L. G.; Clark, J. R.; Parkin, B. C.; Fanwick, P. E.; Rothwell, I. P. *J. Chem. Soc., Dalton Trans.* **1997**, 3353. (c) Riley, P. N.; Thorn, M. G.; Vilardo, J. S.; Lockwood, M. A.; Fanwick, P. E.; Rothwell, I. P. *Organometallics* **1999**, *18*, 3016. (d) Scheiger, S. W.; Salberg, M. M.; Pulvirenti, A. L.; Freeman, E. E.; Fanwick, P. E.; Rothwell, I. P. *J. Chem. Soc., Dalton Trans.* **2001**, 2020.

(10) Fox, P. A.; Bruck, M. A.; Gray, S. D.; Gruhn, N. E.; Grittini, C.; Wigley, D. E. *Organometallics* **1998**, *17*, 2720.

(11) A tantalum tris(ethoxide) complex of an amine bis(phenolate) ligand featured a N–Ta bond length of 2.40 Å (Tshuva, E. Y. Unpublished results).

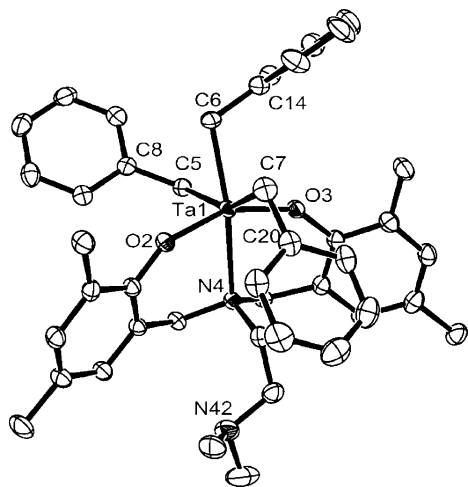


**Figure 3.** ORTEP drawing of **4a** (50% probability ellipsoids). The hydrogen atoms and the crystallization solvent were omitted for clarity. Selected bond distances (Å) and angles (deg): Ta1–O2 = 1.876(2), Ta1–O3 = 1.893(2), Ta1–N4 = 2.513(3), Ta1–C5 = 2.248(3), Ta1–C6 = 2.279(3), Ta1–C7 = 2.250(3); O2–Ta1–O3 = 153.69(10), C6–Ta1–N4 = 165.69(11), C5–Ta1–C7 = 152.17(13).

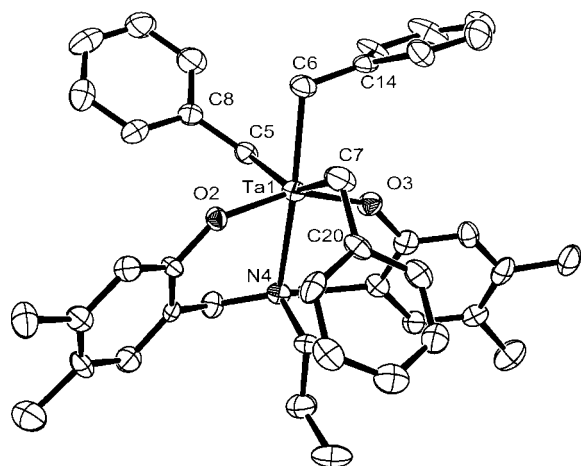
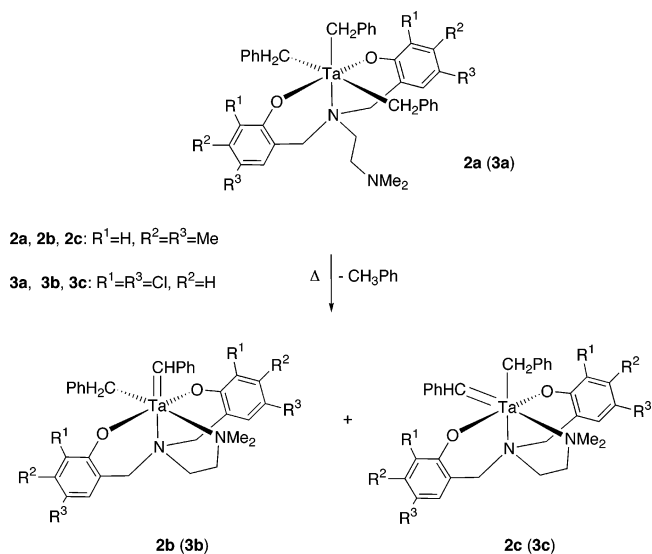


**Figure 4.** ORTEP drawing of **6a** (50% probability ellipsoids). The hydrogen atoms and the crystallization solvent were omitted for clarity. Selected bond distances (Å) and angles (deg): Ta1–O2 = 1.893(5), Ta1–O3 = 1.877(5), Ta1–N4 = 2.548(6), Ta1–C5 = 2.299(7), Ta1–C6 = 2.234(7), Ta1–C7 = 2.203(7); O3–Ta1–O2 = 152.6(2), C5–Ta1–N4 = 164.2(2), C7–Ta1–C6 = 150.3(3).

donating benzyl groups. It is possible that this weak Ta–N bond undergoes detachment in solution, giving rise to the formation of a pseudo-pentacoordinate species, which facilitates the equilibration of the benzyl groups.

The Ta–C bond lengths and the Ta–C–C bond angles are in the ranges of 2.203(7)–2.299(7) Å and 100.5(2)–125.8(5)°, supporting  $\eta^1$  binding. Interestingly, these crystal structures are almost superimposable, except for the slight deviation of the benzyl groups and the N substituent. Noteworthy is the orientation of the “middle” benzyl ligand, i.e., the one trans to the nitrogen donor, which points toward the ortho substituent of the phenolate ring. Probably, this steric interaction for a bulkier substituent in the ortho position (e.g. *t*-Bu) is too severe, thus preventing the formation of tribenzyl complexes

### Scheme 2 $\alpha$ -Abstraction Process Leading to Alkyl–Alkylidene Complexes



with amine bis(phenolate) ligands featuring *t*-Bu substituents on the two phenolate rings.

**Formation and Structure of Alkylidene Complexes.** The conditions known to facilitate alkylidene formation via  $\alpha$ -hydrogen abstraction are (1) sufficient steric bulk around the metal and (2) addition of an “external donor”, such as the small ligand PMe<sub>3</sub>.<sup>1,2c</sup> A priori, it would seem plausible that an “internal donor”, covalently bonded to a ligand, will have the same, or even greater, effect on the formation of an alkylidene group. However, the role of such an internal donor has been much less explored.<sup>12</sup> The tribenzyl complexes **2a**–**5a** presented above contain such a “dormant” internal donor, unattached to the metal. We anticipated that, under certain conditions, this donor would be able to trigger the  $\alpha$ -hydrogen abstraction sequence and lead to the alkyl–alkylidene complexes.

Upon heating of **2a** or **3a** to ca. 90 °C, a fast reaction takes place, leading to a mixture of two alkyl–alkylidene products for both substrates (**2b** and **2c** and **3b** and **3c**, respectively; see Scheme 2), accompanied by liberation of toluene. The relative ratios of the products are different for **2a** and **3a**, being ca. 3:1 and 1.5:1, respectively. The existence of a Ta=C double bond in these species is clearly manifested by <sup>1</sup>H NMR (9.18 and 9.28 ppm for **2b** and **2c**, 8.95 and 8.80 ppm for **3b** and **3c**), and <sup>13</sup>C NMR (247.2 ppm for both **2b** and **2c**, 249.0 and 249.2 ppm for **3b** and **3c**). In addition to the benzylidene signal, the <sup>1</sup>H NMR spectrum of each complex contains two types of ligand aromatic protons, a single AB system for the Ar–CH<sub>2</sub>–N protons, and a sharp singlet for the PhCH<sub>2</sub> protons. According to the <sup>1</sup>H and <sup>13</sup>C NMR spectra, the two products resulting from each starting material are structural isomers of presumably C<sub>s</sub> symmetry (on the NMR time scale at room temperature). This isomerism could stem from binding of the side-arm donor to the metal, with the alkylidene ligand and the dimethylamino donor mutually cis or trans (see Scheme 2). There is no intercon-

(12) Van Doorn, J. A.; van der Heijden, H.; Orpen, A. G. *Organometallics* **1994**, *13*, 4271.

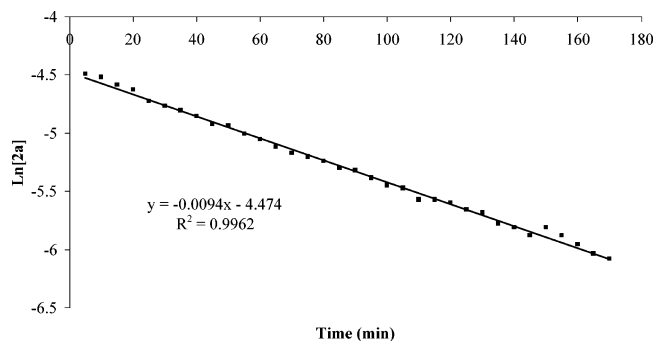


**Figure 5.** Decomposition of **3a**.

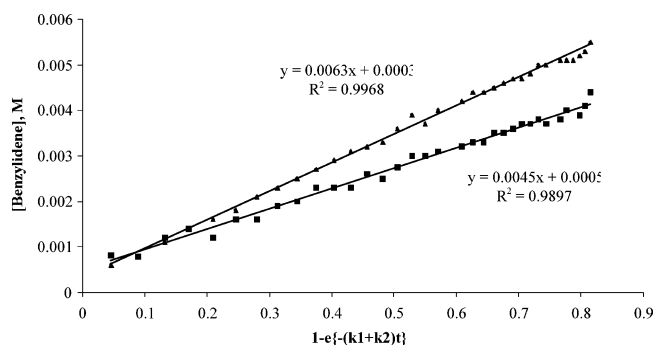


**Figure 6.** Formation of the two benzylidene isomers (**3b** and **3c**) upon **3a** decomposition.

version between the **2b–2c** and **3b–3c** isomers upon heating: that is, they are stable on the laboratory time scale.

To obtain further insight into the reaction mechanism, we followed the decomposition of **3a** at 54(1) °C by means of <sup>1</sup>H NMR spectroscopy, in the presence of an internal standard compound (Me<sub>3</sub>Si–O–SiMe<sub>3</sub>). The reaction (**3a** → **3b** + **3c** + toluene) follows a first-order kinetics, as expected for the α-hydrogen abstraction reaction (see Figure 5 for details).<sup>1–3</sup> The observed rate of decomposition of **3a**, 1.6 × 10<sup>−4</sup> s<sup>−1</sup>, is of the same order of magnitude as the rate constant reported for the decomposition of pentabenzyltantalum (0.4 × 10<sup>−4</sup> s<sup>−1</sup> at 40 °C).<sup>2b</sup> Significantly, the total concentration of the reactant and both products is equal to the initial concentration of **3a** throughout the reaction, implying that no other organometallic product is formed except for the two alkyl–alkylidene complexes. The reaction clearly obeys a C ← A → B reaction sequence (Figure 6), giving further evidence that the isomers do not interconvert under the reaction conditions employed and yielding partial rate constants of  $k_1 = 0.9 \times 10^{-4} \text{ s}^{-1}$  and  $k_2 = 0.6 \times 10^{-4} \text{ s}^{-1}$ , for **3b** and **3c**, respectively.<sup>13</sup> Similarly, the observed decomposition of **2a** at 54(1) °C is also first order in [Ta], with a rate constant of 1.3 × 10<sup>−4</sup> s<sup>−1</sup>.

The major isomer of each reaction mixture (**2b** and **3b**) could be isolated by partial crystallization. The yield for the isolation of pure **2b** is low (22%), despite the favorable product ratio, perhaps due to its high solubility in hydrocarbon solvents. Fortunately, pure **3b** is obtained in good yield upon crystallization from toluene solution (several crops). **3b** may be synthesized directly, in a one-pot synthesis, from Lig<sup>3</sup>H<sub>2</sub> and Ta(CH<sub>2</sub>Ph)<sub>5</sub> (see

Experimental Section for details) in an overall yield of 44%. X-ray structure determination was carried out for both compounds (Figures 7 and 8).

Significantly, the major isomers **2b** and **3b** have the same configuration. Both compounds are alkyl–alkylidene Ta(V) complexes, with the side-arm donor attached to the metal, thus completing its octahedral geometry. The benzyl ligand is located trans to the side-arm donor, and the benzylidene ligand is trans to the central nitrogen. Except for the attachment of the donor, the coordination mode of the amine bis(phenolate) ligand core ([ONO]) remained unchanged. The tantalum–carbon single- and double-bond lengths differ markedly, being 2.246(8) Å vs 1.968(10) Å for **2b** and 2.256(3) Å vs 1.992(4) Å for **3b**. Interestingly, the side-arm nitrogen is bound more tightly to the metal than the central nitrogen (**2b**, 2.402(7) Å vs 2.567(10) Å; **3b**, 2.385(2) Å vs 2.497(3) Å, respectively). This may be attributed to a stronger trans effect of an alkylidene relative to an alkyl ligand.<sup>14</sup> The relatively small distortion of the benzylidene ligand (Ta=C–C bond angle of 140.7(7)° for **2b** and 143.0(3)° for **3b**) is consistent with the relatively large value of 106 Hz for <sup>1</sup>J<sub>C–H</sub> (measured for **3b**) and denotes a weak α-gostic interaction.<sup>1</sup>

The orientation of the benzylidene ligand deserves some attention (see Figures 7 and 8). The C(8)–C(6)–Ta unit of the benzylidene ligand in both structures lies in the plane defined by the two phenolic oxygen donors and the central nitrogen donor, with a slight “out of plane” distortion for **3b**. The preference for this orientation may be attributed to competition with the phenolate oxygen lone pairs for empty Ta(dπ) orbitals to which electron donation can take place: by turning “sideways”, the alkylidene carbon p orbital may π-interact with a specific Ta d orbital that cannot interact with the oxygen lone pairs due to symmetry considerations, as shown in Figure 9. The slight “out of plane” distortion of the alkylidene ligand in **3b** (see top view in Figure 8) may result from steric interaction with the ortho-positioned chloro group, which is consistent with a slight elongation of the Ta=C bond in **3b**.

**Role of the Ortho Substituents: C–H Activation of the Ligand Backbone.** Upon heating, the reaction takes different paths for **4a** and **5a**. <sup>1</sup>H and <sup>13</sup>C NMR spectra of the crude reaction mixtures revealed that only traces of alkylidene products have formed. Instead, the major product in both reactions (**4b** and **5b**) was a dibenzyl complex of low (C<sub>i</sub>) symmetry, as evident from four different Ar–Me groups.

So far, our attempts to obtain pure **4b** have failed; however, the crude reaction mixtures containing **4b** and **5b** are similar. Complex **5b** could be isolated in a pure form by crystallization from cold ether as deep yellow plates. The crystals obtained were subjected to X-ray diffraction study, revealing an unusual heptacoordinate complex of approximately pentagonal-bipyramidal geometry around the Ta center (see Figure 10). A benzyl carbon on the ligand backbone has been activated,

(13) Alberty, R. A.; Silbey, R. J. *Physical Chemistry*; Wiley: New York, 1991.

(14) (a) Abbenhuis, H. C. L.; van Belzen, R.; Grove, D. M.; Klomp, A. J. A.; van Mier, G. P. M.; Spek, A. L.; van Koten, G. *Organometallics* **1993**, *12*, 210. (b) Rietveld, M. H. P.; Teunissen, W.; Hagen, H.; van der Water, L.; Grove, D. M.; van der Schaaf, P. A.; Mühlebach, A.; Kooijman, H.; Smeets, W. J. J.; Veldman, N.; Spek, A. L.; van Koten, G. *Organometallics* **1997**, *16*, 1675. (c) Abbenhuis, H. C. L.; Rietveld, M. H. P.; Haarman, H. F.; Hogerheide, M. P.; Spek, A. L.; van Koten, G. *Organometallics* **1994**, *13*, 3259.

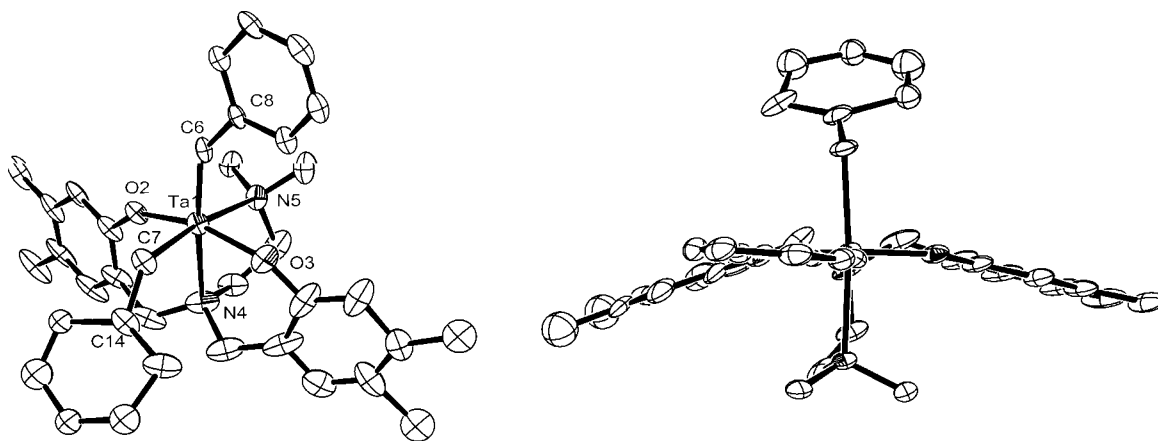


**Figure 7.** ORTEP drawings of **2b** (side view (left) and top view (right); 30% probability ellipsoids). Only one conformation of the disordered benzyl ligand is shown. Hatoms are omitted for clarity. The structure of **2b** was of somewhat low quality, because the diffraction data of the partly twinned crystals could not be well resolved. This is mostly reflected in the elongated ellipsoids of the phenolate rings. Selected bond distances (Å) and angles (deg): Ta1–O2 = 1.883(7), Ta1–O3 = 1.894(8), Ta1–N4 = 2.402(7), Ta1–N5 = 2.567(10), Ta1–C6 = 1.968(10), Ta1–C7 = 2.246(8); C8–C6–Ta1 = 140.7(7).

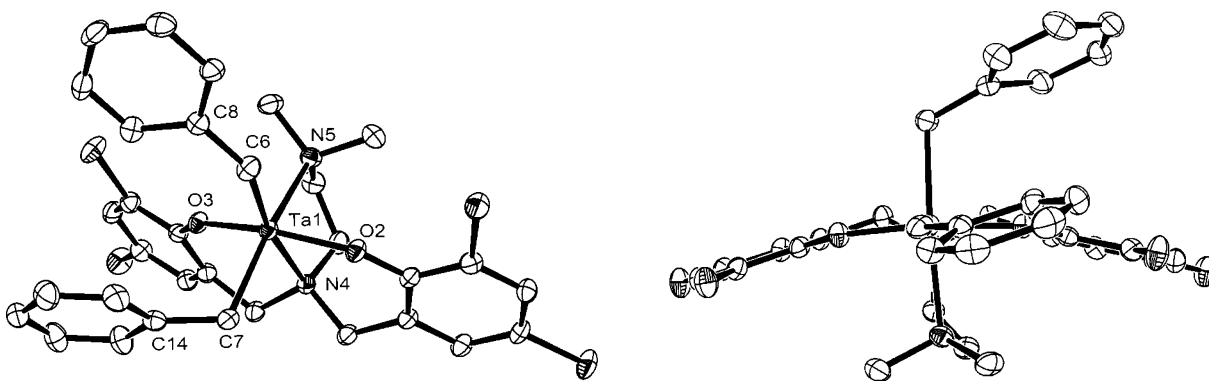


**Figure 8.** ORTEP drawing of **3b** (side view (left) and top view (right); 50% probability ellipsoids). H atoms and toluene solvent are omitted for clarity. Selected bond distances (Å) and angles (deg): Ta1–O2 = 1.935(2), Ta1–O3 = 1.924(2), Ta1–N4 = 2.385(2), Ta1–N5 = 2.497(3), Ta1–C6 = 2.256(3), Ta1–C7 = 1.992(4); O3–Ta1–O2 = 157.79(9), C6–Ta1–N4 = 164.31(10), C7–Ta1–N5 = 167.73(11), C8–C7–Ta1 = 143.0(3), C14–C6–Ta1 = 113.1(2), C20–O2–Ta1 = 145.4(2), C37–O3–Ta1 = 145.75(19).

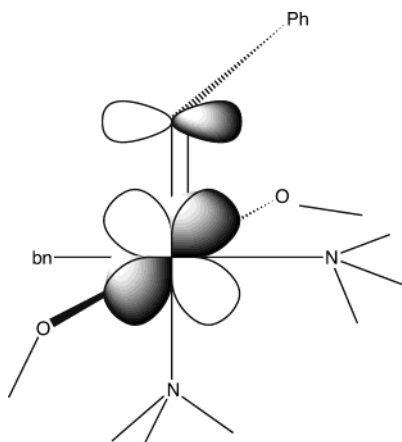


**Figure 9.** Sideways bending of the benzylidene group dictated by a specific  $\pi\pi$ – $d\pi$  interaction.

leading to pentacoordinate binding of the amine bis(phenolate) ligand to the metal center. This is our first encounter with such an activation of the amine bis(phenolate) ligand backbone, which thus far seemed to be highly robust. According to the bond lengths and angles, the formed metallacyclopropane ring contains the neutral nitrogen  $\sigma$ -donor tightly bound to the metal (Ta1–N5 = 2.188(4) Å), along with the alkyl donor

(Ta1–C6 = 2.251(5) Å). This ring resembles those reported for the Ta complexes with arylamine ligands.<sup>14,15</sup> Both phenolate oxygen donors occupy axial positions (O2–Ta1–O3 = 164.95(15)°). The Ta–OAr bond lengths are longer in **5b** (1.944(3) and 1.980(3) Å) than in the tribenzyl (1.876(2)–1.916(2) Å) complexes and the benzyl–benzylidene (1.883(7)–1.935(2) Å) complexes, and the Ta–O–C bond angles are substantially narrower (124.9(3) and 131.8(3)°) than in the tribenzyl complexes (144.9(2)–148.8(2)°) and the benzyl–benzylidene complexes (143.5(9)–145.8(2)°). This may result from a reduced O( $p\pi$ )–Ta( $d\pi$ ) electron donation in the hepta-coordinate **5b**.<sup>9a,14c,16,17</sup> The Ta–C bond lengths and Ta–C–C bond angles in **5b** lie in the normal ranges of 2.199(5)–2.271(5) Å and 111.8(4)–119.5(4)°.

The unique decomposition pathway leading to **5b** (and presumably to **4b**), competing with the “normal”  $\alpha$ -hydrogen abstraction process, may be described as “ $\beta$ -hydrogen abstraction”, given the N-to-Ta coordination (see Figure 11). The closest distance between a benzyl carbon and a neighboring “ $\beta$ -H” is ca. 2.9 Å, as revealed

(15) De Castro, I.; Galakhov, M. V.; Gómez, M.; Gómez-Sal, P.; Royo, P. *Organometallics* **1996**, *15*, 1362.

(16) Goffindaffer, T. W.; Rothwell, I. P.; Huffman, J. C. *Inorg. Chem.* **1983**, *22*, 2906.

(17) Wolczanski, P. T. *Polyhedron* **1995**, *14*, 3335.



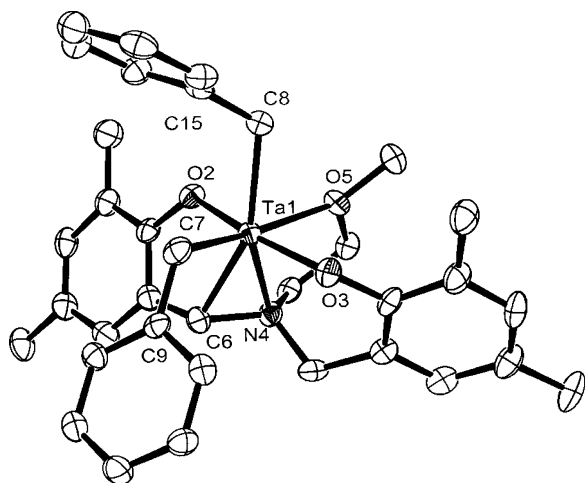


**Figure 10.** ORTEP drawing of **5b** (50% probability ellipsoids). H atoms and disordered solvent are omitted for clarity. Selected bond distances (Å) and angles (deg): Ta1–O2 = 1.980(3), Ta1–O3 = 1.944(3), Ta1–O4 = 2.361(4), Ta1–N5 = 2.188(4), Ta1–C6 = 2.251(5), Ta1–C7 = 2.199(5), Ta1–C8 = 2.271(5); O3–Ta1–O2 = 164.95(15), C7–Ta1–C6 = 87.63(19), N5–Ta1–C6 = 38.92(16), N5–Ta1–O4 = 70.89(14), C8–Ta1–O4 = 82.69(16), C21–O2–Ta1 = 124.9(3), C36–O3–Ta1 = 131.8(3).

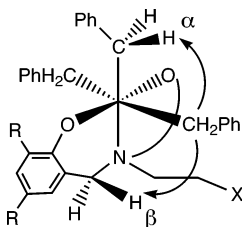


**Figure 11.** Possible decomposition routes for the tribenzyl complexes **2a–7a**.

from the solid-state structure of **4a**, and is only slightly longer than the distance between the active groups leading to the  $\alpha$ -hydrogen abstraction process: i.e., a benzyl carbon and a proton of an adjacent benzyl group of ca. 2.5 Å. Therefore, a competition between these two processes may take place. We propose that this competition is governed by the size of the ortho substituents on the phenolate rings. Notably, certain  $[N_3N]Ta(CH_2R)_2$ -type complexes were found to decompose through a similar  $\beta$ -hydrogen abstraction in the triamido-amine ligand backbone.<sup>18</sup> However, such a pathway in that system triggered a C–N bond scission in the ligand backbone, leading to the formation of tetraamido-monoalkyl derivatives, which contain the Ta–NRCH=CH<sub>2</sub> fragment. Thus, it seems that the use of the aromatic rings as the “spacers” between donor atoms increases the C–N bond stability and leads to the formation of a metallaazacyclopropane ring, instead.

We followed the decomposition of **5a** by <sup>1</sup>H NMR spectroscopy. Since **5a** did not exhibit any significant signs of decomposition at 54 °C for 1 h, the NMR experiments were performed at higher temperatures (65(1), 71(1), and 76(1) °C) in toluene-*d*<sub>8</sub>. At all three temperatures, the reaction mixture during the experiment consisted of at least three distinct organometallic

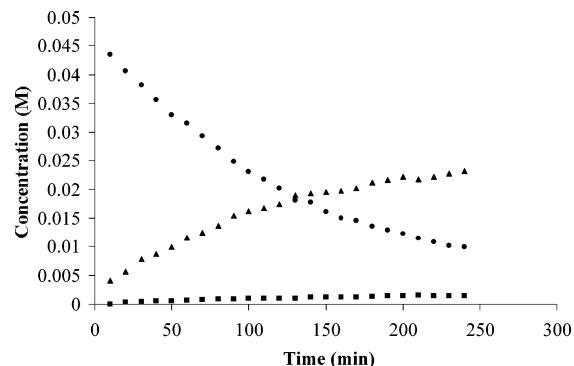


**Figure 12.** Decomposition of **5a**, which leads to the formation of **5b** and **5c** (65 °C; **5c** is represented by the bottom dotted line).

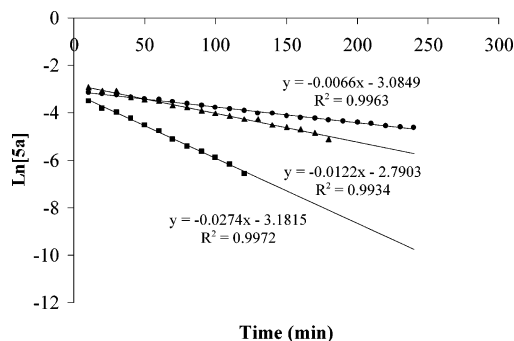


**Figure 13.** First-order decomposition of **5a** at 65, 71, and 76 °C.

species. Along with the starting complex **5a** and the major product **5b**, an additional product, albeit in a low concentration, was detected throughout the experiment (Figure 12). According to the recognizable signal at 9.2 ppm in the <sup>1</sup>H NMR spectrum, this additional product is assumed to be an alkyl-alkylidene complex (of the **2b** and **3b** type).

The decompositions at all the temperatures occurred with first-order kinetics, having rate constants of  $1.1 \times 10^{-4}$ ,  $2.0 \times 10^{-4}$ , and  $4.5 \times 10^{-4}$  s<sup>-1</sup> at 65(1), 71(1), and 76(1) °C, respectively (Figure 13). The low concentration of the presumed benzyl-benzylidene complex **5c**, along with the apparent formation of traces of additional products, does not allow a more detailed kinetic study.

The preference for the  $\beta$ -H abstraction pathway, derived from the steric bulk of an ortho substituent, is even more pronounced in the reaction of Lig<sup>8</sup>H<sub>2</sub> with Ta(CH<sub>2</sub>Ph)<sub>5</sub>. As mentioned above, Lig<sup>1</sup>H<sub>2</sub>, the amine bis(phenolate) ligand precursor, bearing ortho *t*-Bu groups on both phenolate rings, does not react with Ta(CH<sub>2</sub>Ph)<sub>5</sub> at room temperature. The reaction of the “half-bulky” Lig<sup>8</sup>H<sub>2</sub> with Ta(CH<sub>2</sub>Ph)<sub>5</sub>, on the other hand, was found to proceed smoothly, leading to a single product. However, the reaction does not yield the expected tribenzylamine bis(phenolate) Ta(V) complex **8a**. Proton and carbon spectra of the product suggest an asymmetric *dibenzyl* product, possessing no alkylidene signals. The DEPT-135 spectrum displays five different methylene signals, along with a single methine signal, characteristic of the C–H activated product (110 ppm for **8b**, 106 ppm for **5b**). The final confirmation of the nature of **8b** was obtained by means of X-ray crystallography (Figure 14). As a whole, the molecular structure of **8b** resembles the structure of **5b**, including the

(18) (a) Freundlich, J. S.; Schrock, R. R.; Davis, W. M. *J. Am. Chem. Soc.* **1996**, *110*, 4964. (b) Freundlich, J. S.; Schrock, R. R.; Davis, W. M. *Organometallics* **1996**, *15*, 2777.

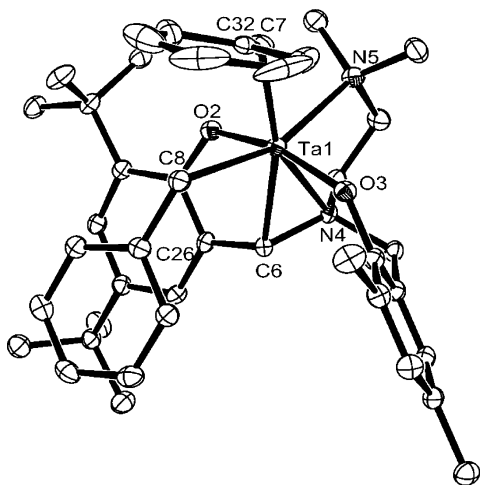


**Figure 14.** ORTEP drawing of **8b** (50% probability ellipsoids). H atoms and the pentane molecule are omitted for clarity. The elongated ellipsoids of one of the phenyl rings reflect the conformational disorder. Selected bond distances (Å) and angles (deg): Ta1–O2 = 1.977(3), Ta1–O3 = 1.928(3), Ta1–N4 = 2.463(4), Ta1–N5 = 2.205(3), Ta1–C6 = 2.246(4), Ta1–C7 = 2.288(4), Ta1–C8 = 2.254(4); O3–Ta1–O2 = 163.68(11), N5–Ta1–C6 = 38.71(12), C6–Ta1–C7 = 165.47(15), N5–Ta1–N4 = 72.86(12).

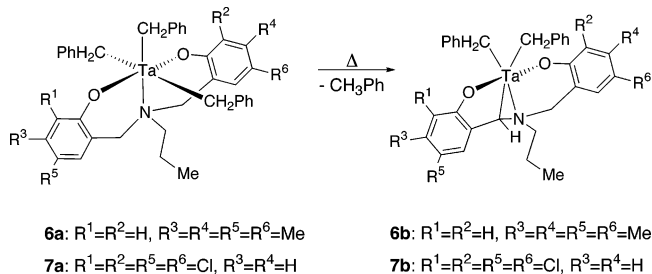
orientation and bond lengths of the corresponding benzyl groups and of the Ta–N–C metallacycle. As in **5b**, the Ta–O bond lengths (1.928(3) and 1.977(3) Å) and Ta–O–C bond angles (123.6(2) and 136.3(2)°) in **8b** indicate a reduced O( $p\pi$ )–Ta( $d\pi$ ) donation, likely due to the existence of the additional donor in this hepta-coordinate complex. Notably, the C–H activation takes place at the more crowded (*t*-Bu carrying) ligand side.

The structure of **8b** supports our proposal that the reaction course is dictated, among other consideration, by the size of the ortho substituents of the phenolate rings. Whereas methyl groups prevent the formation of an alkylidene function upon the thermal decomposition of a tribenzyl precursor, an even stronger steric congestion caused by a single *t*-butyl group leads directly to the C–H activated product. The preference of “ $\beta$ -H abstraction” pathway could be traced back to the tendency of the benzylidene group to point toward the ortho substituent, being hindered as the latter becomes bulky.

**Role of the Side-Arm Donor.** Thus far, we observed that the side-arm donor binds to the metal upon toluene elimination. However, since that binding occurs in both reaction pathways, i.e.  $\alpha$ - or  $\beta$ -H abstraction, the role of this “intramolecular” donor in promoting the formation of alkylidene complexes still has to be clarified. Given the tendency of the tribenzyl Ta complexes of amine bis(phenolate) ligands with “compact” ortho substituents (H in **2a**, Cl in **3a**) to lead to benzylidene complexes, the corresponding tribenzyl complexes of the analogous ligands that lack an additional donor (**6a** and **7a**, respectively) were investigated.

When subjected to thermolysis, **6a** and **7a** undergo toluene elimination reactions, affording a single *dibenzyl* product for each reactant (**6b** and **7b**, respectively). According to the  $^1\text{H}$  NMR spectra, no benzylidene complex is detected upon decomposition of **7a** and only traces are observed on decomposition of **6a**. Notably, the

### Scheme 3. Proposed Structures of **6b** and **7b**



reaction is significantly slower for this type of complexes. Keeping in mind the almost instantaneous decomposition of **2a–5a** at 90 °C, we were surprised to find that ca. 25% of **7a** had not reacted even after 4.5 h at that temperature! The  $^1\text{H}$  NMR monitored decomposition of **6a** at 76(1) °C yielded a rate constant of  $1.7 \times 10^{-4} \text{ s}^{-1}$ , which is significantly lower than the decomposition rate constant of **5a** measured at the same temperature ( $4.5 \times 10^{-4} \text{ s}^{-1}$ ). Complex **7a** did not exhibit any appreciable decomposition at 76(1) °C for ca. 1 h.

Relatively pure **6b** is obtained in moderate yield, albeit after a somewhat tedious workup procedure (see Experimental Section); pure **7b** is obtained upon recrystallization from cold ether (as yellow microcrystals).  $^1\text{H}$  NMR spectra indicate  $C_1$ -symmetrical complexes, possessing three different AB systems (integrated each to two protons), one singlet (integrated to a single proton), and five different Me groups (in **6b**). The  $^{13}\text{C}$  NMR (DEPT) spectra feature a single nonaromatic C–H resonance (80 ppm for **6b**, 77 ppm for **7b**). Again, the low symmetry is confirmed by five different  $\text{CH}_2$  peaks for both complexes, along with five  $\text{CH}_3$  signals for **6b** (a single  $\text{CH}_3$  signal for **7b**). On the basis of the structures of **5b** and **8b**, we propose that **6b** and **7b** are C–H activated hexacoordinate complexes.

Although the  $\beta$ -H abstraction in these complexes is evident, the exact location of the C–H activated carbon needs confirmation. The Ph– $\text{CH}_2$ –N site seems to be the most appropriate. However, the N $\text{CH}_2(\text{CH}_2)$  position cannot be totally excluded, according to the proton spectrum of **6b** and **7b**. The specific location of the activated C–H site was clarified by means of 2D NMR spectroscopy. Since the spectra of **6b** and **7b** seem very much alike, 2D experiments were performed for **6b** only.  $^3J_{\text{H-H}}$  correlation spectroscopy (COSY) unequivocally demonstrated a full correlation pattern for N $\text{CH}_2\text{CH}_2$ – $\text{CH}_3$ , thereby verifying that the propyl unit remains intact. The other correlations detected in the aliphatic region are between diastereotopic  $\text{CH}_2$  protons that appear as three AB patterns. These methylene protons belong to two benzyl ligands and a single Ph $\text{CH}_2\text{N}$  unit. As expected, no correlation was detected for the CH resonance. These results clearly support a “regular”  $\beta$ -H abstraction pathway, which takes place at one of the Ph $\text{CH}_2\text{N}$  units. An additional support of the proposed structure of **6b** and **7b** was obtained by a 2D  $^1J_{\text{C-H}}$  correlation experiment (HMQC technique), showing a correlation between the proton singlet at 2.78 ppm and the methine carbon at 80 ppm. Thus, one can safely conclude that the tribenzyl complexes lacking the “intramolecular donor” (**6a** and **7a**) tend to decompose via the  $\beta$ -H abstraction route, as depicted in Scheme 3.

### Conclusions

Our findings indicate that tribenzyltantalum complexes of the chelating amine bis(phenolate) ligands may undergo two well-defined toluene elimination reactions. The preference for either of these two reaction paths is dictated by the steric influence of the phenolate substituents and the presence of an extra donor on the side arm. As the benzylidene group prefers to point at a specific direction, it should come as no surprise that, by hindering this specific direction via bulky ortho substituents on the phenolate rings, the  $\alpha$ -hydrogen abstraction pathway is blocked and replaced by the competitive  $\beta$ -hydrogen abstraction pathway.

The source of the side-arm donor dependence of the  $\alpha$ -hydrogen abstraction pathway is less obvious. The trialkyl complexes of amine bis(phenolate) ligands lacking the side-arm donor are substantially more stable, and when they eventually do react, they choose the  $\beta$ -hydrogen abstraction path, even in the absence of

steric hindrance. Possible explanations for this dependence may be either of a kinetic source, e.g. a requirement of side-arm coordination prior to  $\alpha$ -hydrogen abstraction, or a thermodynamic source, e.g. the instability of a five-coordinate benzyl–benzylidene tantalum complex of this ligand system. We are currently investigating the reactivity of these types of complexes.

**Acknowledgment.** This research was supported by the Ministry of Science, Culture and Sport and by the Israel Science Foundation, founded by the Israel Academy of Sciences and Humanities. S.G. thanks Sheba D. Bergman for technical assistance.

**Supporting Information Available:** Crystallographic data as CIF files for **3a**, **6a**, **2b**, **3b**, **5b**, and **8b**. This material is available free of charge via the Internet at <http://pubs.acs.org>.

OM0499761